

This is an Open Access document downloaded from ORCA, Cardiff University's institutional repository: <https://orca.cardiff.ac.uk/id/eprint/179208/>

This is the author's version of a work that was submitted to / accepted for publication.

Citation for final published version:

Jia, Ru, Wang, Yu, Wang, Huachao, Ji, Xiao, Sadiq, Faizan Ahmed, Wang, Xu and Zhang, Guohua 2025. The role of quorum sensing effector ComA in regulating biofilm formation and surfactin production in *Bacillus subtilis* ASAG 010. *Food Bioscience* 69, 106842. 10.1016/j.fbio.2025.106842

Publishers page: <http://dx.doi.org/10.1016/j.fbio.2025.106842>

Please note:

Changes made as a result of publishing processes such as copy-editing, formatting and page numbers may not be reflected in this version. For the definitive version of this publication, please refer to the published source. You are advised to consult the publisher's version if you wish to cite this paper.

This version is being made available in accordance with publisher policies. See <http://orca.cf.ac.uk/policies.html> for usage policies. Copyright and moral rights for publications made available in ORCA are retained by the copyright holders.



**The Role of Quorum Sensing Effector ComA in Regulating Biofilm Formation and Surfactin**

**Production in *Bacillus subtilis* ASAG 010**

Ru Jia <sup>a,\*</sup>, Yu Wang <sup>a</sup>, Huachao Wang <sup>a</sup>, Xiao Ji <sup>a</sup>, Faizan Ahmed Sadiq <sup>b</sup>, Xu Wang <sup>a</sup>, Guohua Zhang <sup>a</sup>

<sup>a</sup>*School of Life Science, Shanxi University, 92 Wucheng Road, Taiyuan 030006, China*

<sup>b</sup>*Advanced Therapies Group, School of Dentistry, Cardiff University, CF14 4XY, Cardiff, Wales, UK*

---

\* Corresponding author. School of Life Science, Shanxi University, 92 Wucheng Road, Taiyuan 030006, China. E-mail address: [sxdxjiaru@sxu.edu.cn](mailto:sxdxjiaru@sxu.edu.cn). Tel: 0086-0350-7011274. Fax: 0086-0350-7011274.

**Abstract:** *Bacillus* species are valuable agents in biocontrol and sustainable agriculture. This study focuses on the properties of *Bacillus subtilis* ASAG 010, a strain isolated from wheat-associated soil, which exhibited potent antifungal activity against multiple plant pathogens, including *Fusarium graminearum*. The strain effectively controlled *Fusarium* head blight in wheat and demonstrated the ability to degrade the mycotoxin zearalenone (ZEN). High-performance liquid chromatography (HPLC) and MALDI-TOF-MS analyses, coupled with genetic verification, identified surfactin as the primary antifungal compound produced by *B. subtilis* ASAG 010. Analysis of the static fermentation process revealed that a mature biofilm structure significantly enhanced surfactin synthesis in *B. subtilis* ASAG 010. To investigate the interplay between quorum sensing (QS), biofilm formation, and surfactin production, a *ComA*-deficient mutant was constructed. The mutant exhibited reduced extracellular polysaccharides, proteins, and  $\gamma$ -PGA – key biofilm matrix components – and lower expression of *EpsA* and *BlsA*. HPLC analysis showed a significantly reduced in surfactin production, and DNA pull-down assays confirmed that *ComA* directly binds upstream of the *urfA* gene, which encodes surfactin biosynthesis. These findings establish ComA as a key regulator of biofilm integrity and surfactin production, providing insights into the biocontrol potential of *B. subtilis* ASAG 010 for food safety and agricultural sustainability.

**Keywords:** *Bacillus subtilis*, Surfactin, Biofilm, Quorum sensing, Zearalenone

## 1. Introduction

*Fusarium graminearum* is the primary fungal pathogen responsible for *Fusarium* head blight (FHB) in wheat (Johns *et al.*, 2022) and significantly impacts the yield and quality of other major crops, including rice and maize (Fruhauf *et al.*, 2024), posing serious threats to agricultural economies and food safety. Control methods for *F. graminearum* primarily encompass chemical treatments, agricultural practices, and biological approaches. Among these, biological control stands out as a promising alternative due to its safety, environmental sustainability, and effectiveness in managing plant pathogens (Kimotho *et al.*, 2024).

Biological control of plant pathogens is a sustainable agricultural strategy that employs beneficial microorganisms or their metabolites to inhibit or suppress the growth and spread of plant diseases, promoting crop health in an environmentally friendly manner (Borriss *et al.*, 2023). Common biocontrol methods include the use of probiotics (Harutyunyan *et al.*, 2022), actinomycetes (Ebrahimi-Zarandi *et al.*, 2022), fungi (Thambugala *et al.*, 2020) and other biological entities to combat plant pathogenic microorganisms. In particular, certain bacteria, such as *Bacillus*, have been extensively studied and applied in the biocontrol of plant diseases due to their broad-spectrum antibacterial activity (Zhang *et al.*, 2023). These bacilli – which are often probiotic in nature – exert their biocontrol effects through various mechanisms, including competitive exclusion of pathogens (Lahlali *et al.*, 2022), the production of antimicrobial substances (Dimkić *et al.*, 2022), the enhancement of plant disease resistance (Guo *et al.*, 2017), quorum quenching to disrupt pathogen communication (Cheng *et al.*, 2024), and the induction of plant growth-promoting hormones (Jensen *et al.*, 2024). Among these mechanisms, antimicrobial substances have become a major focus of biocontrol research due to their broad spectrum of activity, high efficacy, structural diversity, and

varied modes of action. Additionally, their relative environmental safety, potential for sustainable agricultural practices, and ability to target specific pathogens without disrupting beneficial microbiota make them particularly appealing for modern biocontrol strategies (Reveglia *et al.*, 2024). These antimicrobial substances mainly include antibiotics, lipopeptides, and enzymes, which can directly damage the cell wall or membrane of pathogenic microorganisms, thereby inhibiting their growth or inducing pathogen death (Wang *et al.*, 2025). For instance, *Bacillus velezensis* HY19 produces hydrolases that inhibit common fungal pathogens in citrus fruits (Li *et al.*, 2024). Similarly, the fengycin produced by *B. subtilis* FAJT-4 induces early apoptosis in *F. graminearum* cells upon treatment (Deng *et al.*, 2024).

With the in-depth study of antimicrobial peptides and other antimicrobial bioactive substances, the factors influencing their biosynthesis have also gained attention. Research has shown that the synthesis of specialized metabolites many biocontrol agents is primarily influenced by external factors such as nutritional conditions (Bisht *et al.*, 2020), temperature, pH, internal factors that encompass genetic regulation (Miao *et al.*, 2024) and transcriptional control mechanisms, and microbial interactions (Sun *et al.*, 2021). Biofilm formation is an important phase of microbial life during which their metabolic state is significantly different from the planktonic state evident from changes in metabolic profile and stress responses (Sadiq *et al.*, 2020). Thus, bacteria may produce different levels of metabolites when grown in biofilms compared to their planktonic state (Wong *et al.*, 2018). A biofilm is a structured microbial community (Arnaouteli *et al.*, 2021a) that, compared to planktonic cells, exhibits greater resilience to harsh conditions and facilitates both cooperative and competitive interactions among its members (Yao *et al.*, 2022). These interactions can drive the elevated production of metabolites with significant biocontrol potential, highlighting the adaptive advantages of biofilm-based lifestyles in

microbial systems (Jiang *et al.*, 2021). For instance, the biofilm of *Clostridium beijerinckii* achieves an acetone-butanol-ethanol yield of 15.8 g/L/h, which is approximately 50 times higher than that of typical planktonic cells (Liu *et al.*, 2014). *Corynebacterium glutamicum* continuous fermentation based on biofilm has a production advantage in L-lysine yield compared to traditional free-cell fermentation (Peng *et al.*, 2024). Robust biofilm formation could enhance MK-7 biosynthesis in *B. subtilis natto* (Yi *et al.*, 2024).

Quorum sensing (QS) serves as a fundamental mechanism of community-level communication within biofilms, allowing bacteria to detect and respond to signaling molecules that regulate gene expression and orchestrate collective behaviors essential for biofilm formation and maintenance (Whiteley *et al.*, 2017). For instance, both *Gram*-positive and *Gram*-negative bacteria can use the QS system to regulate the synthesis of surface structures (Wang *et al.*, 2022), thereby initiating or enhancing biofilm formation. In addition to its impact on biofilm formation, QS system also plays a role in regulating important physiological processes in microbes, such as antibiotic synthesis (Zhou *et al.*, 2023) and the production of metabolic compounds (Wu *et al.*, 2022).

To effectively control wheat FHB and the occurrence of zearalenone (ZEN) at the source, we isolated *B. subtilis* ASAG 010 from wheat-associated soil, a strain exhibiting both pathogen antagonism and ZEN degradation capabilities. In addition, we investigate how the biofilm state and structure of *B. subtilis* ASAG 010 influence surfactin production and how QS is implicated in this process. We hypothesize that surfactin production in *B. subtilis* is modulated by the biofilm state and is regulated by QS-controlled mechanisms. In this study, we first investigated the impact of biofilm structure on surfactin synthesis in *B. subtilis*. To further explore the role of QS in biofilm formation, we constructed a *ComA*-deficient mutant strain using homologous recombination. Finally, the mechanism

by which QS regulates surfactin synthesis was elucidated at both gene and protein levels through RT-qPCR and DNA pull-down assays. These findings provide new insights into strategies for enhancing the synthesis yield of *B. subtilis*-derived and other microbial antibiotics, while laying a foundation for the potential application of *B. subtilis* ASAG 010 as a novel feed additive to combat FHB and ZEN contamination in food and feed.

## 2. Materials and methods

### 2.1. Isolation and identification of antagonistic strains

Soil samples collected from the wheat growth environment were suspended in phosphate-buffered saline (PBS, pH 7.4) and thoroughly well. A 1 mL aliquot of the suspension was diluted and incubated in Luria-Bertani (LB) broth at 37°C with shaking (200 rpm) for 48 h. Single colonies with different morphologies were isolated by streaking on LB agar plates. Antagonistic activity of purified colonies was tested on potato dextrose agar (PDA) plates by placing a 5-mm *F. graminearum* mycelial disk at the center and inoculating the test colonies 25 mm away. The inhibition rate was determined using the formula (1):

$$\text{Inhibition rate (\%)} = [(C - T) \times 100] \div C \quad (1)$$

C represents the control group, measuring the normal growth mycelium radius, while T represents the treatment group, measuring the inhibited growth mycelium radius (cm).

The strain with the highest inhibition rate was characterized by gram staining, morphological observation, and 16S rRNA sequencing. The 16S rRNA was amplified using primers 27F and 1492R under the following PCR conditions: 94°C for 5 min, 30 cycles of 94°C for 30 s, 50°C for 30 s, and 72°C for 1.5 min, followed by 72°C for 10 min. The amplified products were sequenced (Sangon Biotech, Shanghai, China), and sequences were compared with those in the NCBI database via BLAST

to identify the genus. Phylogenetic trees were constructed using MEGA 11.0 software.

### 2.2. Antifungal activity of the strain fermentation broth on *F. graminearum* mycelium

To examine the ultrastructural changes in *F. graminearum* hyphae following treatment with strain ASAG 010, a scanning electron microscope (SEM, JSM-7001F, JEOL Ltd., Japan) was employed. Hyphae were collected after a 24-h exposure to the fermentation broth of strain ASAG 010. The samples were fixed with 2.5% glutaraldehyde at room temperature of 25 °C for 1.5 h, followed by dehydration through a graded ethanol series. Critical point drying was performed for 1 h, after which the samples were sputter-coated with gold particles. The morphological changes were then visualized using SEM

### 2.3. Biocontrol efficiency of the strain fermentation broth on wheat seedling and grain

The disease control efficacy of strain ASAG 010 against *F. graminearum* was evaluated following the method described by Xu et al. with modifications (Xu *et al.*, 2022). Wheat seedlings with uniform growth were divided into four groups (30 seedlings per group), washed with sterile water, and placed in 9-cm petri dishes. Three treatment groups were sprayed with *F. graminearum* conidia suspension ( $10^3$  CFU/mL), while sterile water served as a positive control. One treatment group received the strain ASAG 216 fermentation broth ( $OD_{600} = 2.0$ ), another with the strain ASAG 010 fermentation broth ( $OD_{600} = 2.0$ ), and the third group, without treatment, served as a negative control. Seedlings were incubated at 22°C for 10 days, after which disease symptoms and coleoptile lesion lengths were recorded.

For wheat grains, 50 g of grains were soaked in sterile water for 24 h and sterilized at 121°C for 20 min. *F. graminearum* conidia suspension ( $10^3$  CFU/mL) and the strain ASAG 010 fermentation broth ( $OD_{600} = 2.0$ ) were prepared. The grains were divided into six groups (a – f). Except for group c, which

was treated with sterile water alone, all groups were inoculated with 1 mL of *F. graminearum* conidia suspension. Group c received 1 mL of LB medium, while groups d, e, and f were supplemented with 0.5 mL, 1 mL, and 2 mL of stain ASAG 010 fermentation broth, respectively. All treatments were incubated at 28°C, and mycelial growth was recorded on the 5th, 10th, 15th, 20th, and 30th days.

#### *2.4. Separation and identification of antifungal substances*

The active antifungal component was extracted from the fermentation broth of strain ASAG 010 using an acid precipitation method. The broth was centrifuged at 8000 g for 20 min at 4 °C to separate the supernatant, which was then adjusted to pH 2 using 6 mol/L hydrochloric acid and incubated at 4°C overnight. The precipitate was collected by centrifugation at 8000 g for 30 min at 4°C, dissolved in methanol, concentrated at 45°C using a rotary evaporator, and dried in a 65°C oven to yield a yellow crude extract.

The crude extract was analyzed using matrix-assisted laser desorption/ionization time-of-flight mass spectrometry (MALDI-ToF-MS Biotyper, Bruker Daltonics, Germany) to determine its molecular mass. The analysis was conducted in positive ion detection mode, with 2,5-dihydroxybenzoic acid (DHB) as the matrix. Desorption and ionization were performed using a UV laser (337 nm wavelength) at a voltage of 20 kV. The mass-to-charge ( $m/z$ ) ratios were measured in the range of 100-1700. The ion source voltages were set to 20 kV (first source) and 17.65 kV (second source), and laser irradiance was maintained at 50-55%. Data were processed and analyzed using FlexAnalysis software (Bruker Daltonics, Bremen, Germany).

#### *2.5. ZEN degradation by the B. subtilis ASAG 010*

To evaluate the ability of *B. subtilis* ASAG 010 to degrade ZEN, 50 µL of ZEN standard solution (10 µg/mL) was mixed with 900 µL of the *B. subtilis* ASAG 010 bacterial suspension or liquid culture

medium, with LB medium serving as the control. The mixtures were incubated at 37°C for 48 h and centrifuged at 8000 g for 5 min. A 1-mL aliquot of the supernatant was collected and passed through an immune affinity column before being diluted with the mobile phase.

ZEN was quantified using high-performance liquid chromatography (HPLC; Shimadzu LC-10AT, Tokyo, Japan) equipped with a Myco-C18 column (4.6 mm × 250 mm, 5 μm, Beijing, China). The mobile phase consisted of acetonitrile, water, and methanol in a ratio of 46:46:8 (v/v/v), with a flow rate of 0.5 mL/min. Injection volumes ranged from 20 to 100 μL. Detection was performed using a fluorescence detector (Shimadzu RF-20A) at an excitation wavelength of 360 nm and an emission wavelength of 440 nm.

#### *2.6. Determination of biofilm biomass, cellular biomass, and surfactin yield*

The activated bacterial culture was inoculated into Landy medium at a 1% (v/v) ratio and incubated statically at 37°C for a defined period. Biofilm biomass was quantified using the crystal violet (CV) staining method. The biofilm formed at the air-liquid interface was carefully collected washed with distilled water, and stained with 0.4% CV at 25 °C for 30 min. Excess dye was removed, and the biofilm was washed twice with distilled water. The CV-stained biofilm was dissolved in 2 mL 30% acetic acid, and the absorbance was measured at OD<sub>570</sub> nm using a UV-Vis spectrophotometer. To determine viable cellular biomass, a small aliquot of the fermentation broth (100 μL) was serially diluted in a 10-fold gradient using sterile saline solution. Diluted samples (100 μL) were plated onto LB agar plates and incubated overnight at 37°C. Colony counts within the range of 30-300 CFU were recorded, and the viable cell concentration was calculated as colony-forming units per milliliter (CFU/mL) based on the dilution factor.

The measurement of surfactin yield was performed according to the method described by Wang

et al. (2024) with modifications. The yellow precipitate obtained as described in section 2.4 was dissolved in methanol, subjected to ultrasonic extraction, and filtered through a 0.22 µm membrane. A 20 µL aliquot was injected into an HPLC system (Shimadzu LC-16, Tokyo, Japan) equipped with a variable wavelength detector set to 214 nm and a C18 column (4.6 mm × 250 mm; 5 µm; Waters, Ireland). The mobile phase consisted of 10% water and 90% acetonitrile with 0.5% trifluoroacetic acid (TFA). The flow rate was set to 1.0 mL/min, and the column temperature was maintained at 40°C. The total peak area corresponding to three surfactin isoforms was calculated to determine the total concentration based on the standard curve.

### 2.7. Construction of knockout strains

Knockout strains were constructed using the thermo-sensitive plasmid pBSCas9. The primers used in this study are listed in Table S1. The upstream and downstream flanking regions of the *ComA* gene were amplified using the corresponding primers. These fragments, along with the pBSCas9 plasmid containing the *ComA*-specific sgRNA (pBSCas9-*ComA*sgRNA1), were digested with the restriction enzyme Sall and ligated using In-Fusion cloning.

The recombinant plasmid (*ComA* UD-sgCas9) was introduced into *B. subtilis* ASAG 010 via electroporation. Positive colonies were screened using identification primers, and successful integration was confirmed by sequencing. Finally, the temperature-sensitive plasmid was eliminated by culturing at non-permissive temperatures to ensure removal of antibiotic resistance markers.

### 2.8. Determination of exopolysaccharides, protein and γ-polyglutamic acid in biofilm

Biofilms from each group were collected into centrifuge tubes and resuspended in 2 mL of distilled water. The biofilms were disrupted and dissolved using an ultrasonic cell disruptor operating at a probe amplitude of 6, with a power of 250 W, for a duration of 20 min.

The contents of exopolysaccharides (EPS), protein, and  $\gamma$ -polyglutamic acid ( $\gamma$ -PGA) in the biofilm were quantified using established methods. EPS was measured using the phenol-sulfuric acid colorimetric method, protein concentration was determined using a BCA protein assay kit, and  $\gamma$ -PGA content was assessed using the cetyltrimethylammonium bromide (CTAB) method. Detailed procedures followed previously published protocols (Branda *et al.*, 2006; Zhang *et al.*, 2022).

### 2.9. Gene expression analysis by RT-qPCR

Total RNA was extracted using the Bacteria Total RNA Isolation Kit and reverse-transcribed into cDNA using the PrimeScript RT Reagent Kit (Takara, Dalian, China) following the manufacturer's protocols. Real-time quantitative PCR (RT-qPCR) was performed using the CFX96 Real-Time System (Bio-Rad, Hercules, CA, USA) with TB Green PCR Mix (Takara, Dalian, China).

Relative gene expression levels were calculated using the  $2^{-\Delta\Delta CT}$  method, with *ccpA* as the reference gene. All primer sequences used for qPCR analysis are listed in Table S1.

### 2.10. Expression and purification of ComA Protein

The full-length *ComA* gene was amplified using the primers *ComA-F* and *ComA-R*, digested with *KpnI* and *NotI*, and ligated into the pET-32a vector. The recombinant plasmid was verified by sequencing and transformed into *E. coli* BL21 (DE3) for protein expression. The transformed cells were grown overnight at 37°C with shaking at 200 rpm in 20 mL LB broth supplemented with 100  $\mu$ g/mL ampicillin. The overnight culture was diluted 1% into fresh LB medium and incubated for 4 h. Protein expression was induced with 0.5 mM IPTG and further incubated for 6 h at 37°C and 200 rpm.

Cells were harvested by centrifugation (8000 g, 4 °C, 15 min), resuspended in lysis buffer, and disrupted by ultrasonication (2s on, 3s off) for 1 h on ice. The lysate was centrifuged (12,000 g, 4 °C, 20 min) to remove cell debris. The supernatant was purified using Ni-NTA resin (Sangon Biotech,

Shanghai, China) and eluted with 250 mM imidazole. Purified ComA protein was analyzed by SDS-PAGE.

#### *2.11. The Binding of Gene *srfA* and protein ComA by DNA Pull-Down*

The promoter region of the *srfA* gene was amplified using biotinylated specific primers. A mixture of 5 µg biotinylated DNA (promoter probe) and 500 µg ComA protein was incubated on ice for 1 h with 100 µL streptavidin-agarose beads at 4°C. After incubation, the DNA-protein complex was pulled down by centrifugation at 5000 g for 30 s at 4 °C. The supernatant was discarded, and the beads were washed three times with cold PBS. After the final wash, the pull-down complex was suspended in distilled water at 70°C for 3 min to disrupt the streptavidin-biotin interaction. The eluted proteins were analyzed by SDS-PAGE.

#### *2.12. Statistical Analysis*

All experiments were performed in triplicate, and the results are presented as the mean ± standard deviation (SD). Statistical analyses were conducted using GraphPad Prism 9.0 (GraphPad Software, San Diego, CA, USA). The significance of differences between groups was assessed using one-way ANOVA or Student's t-test as appropriate. A p-value < 0.05 was considered statistically significant.

### **3. Results**

#### *3.1. Identification of microorganisms*

A total of 10 antagonistic strains were isolated from 100 soil samples, with inhibition rates ranging from 16.98% to 65.45% (Fig. 1A). Among these, the strain ASAG 010 exhibited the highest inhibition rate of 65.45%. Therefore, the strain ASAG 010 was selected for further analysis. Morphological observation revealed that the ASAG 010 forms white colonies with a rough, wrinkled surface and a slightly raised center (Fig. 1B). Gram staining confirmed that the ASAG 010 is

Gram-positive (Fig. 1D). Sequence analysis of the 16S rRNA gene revealed 99% similarity to *B. subtilis* sD9 (Fig. 1C). In summary, strain ASAG 010 was identified as *B. subtilis* and designated as the *B. subtilis* ASAG 010. The strain has been deposited at the China General Microbiological Culture Collection Center (CGMCC, accession number 26062).

### 3.2. Antifungal activity of ASAG 010

#### 3.2.1. Broad-spectrum antifungal activity of ASAG 010

Strain ASAG 010 demonstrated broad-spectrum antifungal activity, effectively inhibiting the growth of five fungal species from different genera (Fig. 2A). Among these, the highest inhibition rate was observed against *Aspergillus niger*, reaching 67.43%.

#### 3.2.2. Effects of fermentation broth on mycelia of *F. graminearum*

The impact of the bacterial fermentation broth on fungal hyphae was further examined using SEM. In the control group, the hyphal surfaces were smooth, with intact and uniform protoplasts (Fig. 2B). In contrast, hyphae treated with the fermentation broth exhibited roughened surfaces and significant shrinkage, suggesting disrupted physiological functions. These morphological alterations indicate that *B. subtilis* ASAG 010 fermentation broth inhibits fungal growth, likely through damage to the mycelial cell wall or membrane structure.

#### 3.2.3. Biocontrol efficiency of the *B. subtilis* ASAG 010 fermentation broth on wheat seedling and grain

The biocontrol efficacy of *B. subtilis* ASAG 010 fermentation broth against *F. graminearum* infection is presented in Fig. 2C. Compared with the control group, treatment with *B. subtilis* ASAG 010 fermentation broth significantly reduced infection in wheat seedlings ( $P < 0.05$ ), whereas *B. subtilis* ASAG 216 showed minimal effect. The average lesion length on coleoptiles was reduced from 1.82 cm in the control group to 0.21 cm in the ASAG 010 treatment group. These findings demonstrate

that *B. subtilis* ASAG 010 fermentation broth effectively prevents and controls *F. graminearum* infection in wheat seedlings.

In the seed treatment experiment, varying degrees of mycelial growth were observed on wheat seeds in each group that received *F. graminearum* conidia suspension (Fig. 2D). The infection effect of *F. graminearum* was significantly reduced when *B. subtilis* ASAG 010 fermentation broth was added, compared to the control group. As the dosage of *B. subtilis* ASAG 010 increased, the inhibition became more pronounced. When the volume of fermentation broth reached 2 mL, the infection of *F. graminearum* was almost completely inhibited.

### 3.3. Identification of surfactin

The active component was identified by HPLC and MALDI-TOF-MS analyses, and the results from both methods were consistent. As shown in Fig. 3A, MALDI-TOF-MS revealed molecular ion peaks (M+Na)<sup>+</sup> at *m/z* 1030.9, 1044.9, and 1058.9, corresponding to surfactin variants with C13, C14, and C15 fatty acid chains, respectively. The observed 14 Da intervals between these peaks reflect the characteristic differences in the carbon chain lengths of surfactin homologs. Furthermore, the HPLC retention times of the detected peaks matched those reported for surfactin in previous studies.

### 3.4. ZEN degradation by the *B. subtilis* ASAG 010

The ability of *B. subtilis* ASAG 010 to degrade ZEN was evaluated by determining ZEN concentrations using HPLC. As shown in Fig. 3, the ZEN concentration decreased from 593 ng/mL in the control group to 77 ng/mL in the treatment group, corresponding to a degradation rate of 86.95%. These findings demonstrate that *B. subtilis* ASAG 010 effectively degrades ZEN.

### 3.5. Analysis of biofilm biomass, cellular biomass and surfactin yield

The morphological structure of the biofilm evolved dynamically, as shown in Fig. 4A. A thin

white membrane formed within the first 12 h, which developed folds and a gelatinous texture by 24 h. By 36 h, the biofilm's color deepened, and the number of folds and pores increased. At 48 h, the structure collapsed and became noticeably flatter. The biofilm biomass (Fig. 4B) increased steadily, although the production rate declined over time, plateauing at approximately 0.8 g/L by 48 h. Cell biomass (Fig. 4C) exhibited an S-shaped growth curve, with slow accumulation between 12 and 24 hours, rapid growth between 24 and 36 h, and a deceleration after 36 h. Surfactin production (Fig. 4D) rose steadily, with accelerated synthesis between 24 and 36 h, peaking at approximately 1.5 g/L at 48 h.

### *3.6. Effects of ComA Gene deletion on biofilm formation, surfactin production, biofilm matrix components and related gene expression*

The *ComA* gene knockout strain of ASAG 010 was successfully constructed, as shown in Fig. 5, and its characteristics were compared to the wild-type strain. The results showed that the wild-type strain produced 1.35 g/L of surfactin (Fig. 6D), while the mutant strain only yielded approximately 0.10 g/L, representing a more than 10-fold reduction in production ( $p < 0.01$ ), indicating a statistically significant difference between the two strains. Concurrently, the biofilm formation capability of the mutant strain was significantly lower than that of the wild-type strain (Fig. 6E). The composition of the biofilm matrix is shown in Fig. 7A. In the wild-type control group, the concentrations of EPS, protein, and  $\gamma$ -PGA were 6.61 mg/mL, 2.08 mg/mL, and 0.18 mg/mL, respectively. However, in the mutant strain, these values were 1.43 mg/mL, 0.77 mg/mL, and 0.05 mg/mL, respectively. Thus, the biofilm matrix of the mutant strain exhibited significantly lower levels of three major components – EPS, protein, and  $\gamma$ -PGA – compared to the wild-type. RT-qPCR analysis (Fig. 7B) revealed that the expression levels of *EpsA* and *BslA* were significantly ( $P < 0.05$ ) reduced in the *ComA*-deficient strain, while the expression levels of *Spo0A*, *RapC*, and *CodY* were significantly ( $P < 0.05$ ) increased. The

expression of *TasA* remained largely unchanged.

### 3.7. Interaction between ComA protein and the *srfA* gene

The interaction between ComA protein and the *srfA* gene promoter was confirmed through a DNA pull-down assay, as shown in Fig. 8. In Lane 1 (negative control), where no ComA protein was added, no band was observed. In Lane 2 (experimental group), a distinct band was detected, indicating that the ComA protein was successfully captured and eluted by the biotinylated probe. Lane 3 (positive control) shows a band where ComA protein was present without additional treatment, verifying the specificity of the assay.

## 4. Discussion

*B. subtilis* is one of the most extensively studied species within the *Bacillus* genus, renowned for its remarkable capabilities in cell division, biofilm formation, and the production of specialized metabolites (Kovács, 2019). These characteristics also make it a highly promising candidate for the control of fungal pathogens and mycotoxins in feed and food systems. In this study, *B. subtilis* ASAG 010, a bacterial strain isolated from wheat habitat soil, exhibited strong inhibitory activity against the growth of *F. graminearum*. Preliminary screening tests revealed that *B. subtilis* ASAG 010 exhibited antimicrobial activity against a range of plant pathogenic fungi and demonstrated the ability to degrade ZEN. Furthermore, biocontrol experiments on wheat seeds and seedlings indicated that the fermentation broth of *B. subtilis* ASAG 010 reduced the risk of *Fusarium* infection in wheat. These findings underscore the biocontrol potential of *B. subtilis* ASAG 010, which not only inhibits the growth and spread of plant pathogens at the source but also degrades existing toxin levels, converting them into non-toxic or less toxic substances, thus demonstrating great potential for safeguarding food security.

To analyze the active components in the fermentation supernatant of *B. subtilis* ASAG 010, MALDI-TOF/MS was employed. This technique is widely recognized for its high sensitivity and capability to determine ion sequences, making it an effective tool for substance structure identification (Yang *et al.*, 2015). The mass spectrometry results revealed peaks at m/z 1030.9, 1044.9, and 1058.9. When combined with the HPLC elution profile, these findings were consistent with previously reported results, further confirming the identification of the active components. For example, Pyoung *et al.* (2010) reported that the surfactin peak from *B. subtilis* CMB32 appeared within the range of 1016 and 1044, which was also confirmed by Bernat *et al.* (2016). Furthermore, PCR analysis confirmed the presence of the *sfp* gene cluster responsible for surfactin synthesis in the genome of *B. subtilis* ASAG 010. Surfactin, a potent biosurfactant, is known for its ability to reduce the surface and interfacial tension of liquids, solids, and gases (Cappello *et al.*, 2012). In addition to its surfactant properties, surfactin exhibits antibacterial (Dai *et al.*, 2024), antifungal (Krishnan *et al.*, 2019), and antiviral activities (van Eijk *et al.*, 2019) by disrupting the cell membranes of pathogenic microorganisms, inhibiting cell division, interfering with normal cellular metabolism, and facilitating the breakdown of pathogen biofilms (Balan *et al.*, 2019). For example, it has been reported that surfactin induces ROS-mediated mitochondrial apoptosis in *F. graminearum* hyphae to exert its antifungal activity (Liang *et al.*, 2023). Surfactin A was reported to significantly reduce rice false smut by up to 80% (Sarwar *et al.*, 2018). This aligns with the findings of the current study, where the fermentation supernatant of *B. subtilis* ASAG 010 caused the hyphal surface of *F. graminearum* to shrink, wrinkle, and exhibit local rupture and indentation, thereby inhibiting its growth and effectively controlling FHB on wheat seedlings and seeds. The relationship between surfactin A production and the bacterial biofilm state has not been previously analyzed. This study is the first to elucidate how the biofilm state

influences surfactin A production by *B. subtilis* ASAG 010.

To explore the correlation between biofilm formation and surfactin biosynthesis in the metabolic processes of *B. subtilis* ASAG 010, a biofilm fermentation approach was employed (Berenjian *et al.*, 2015). The study analyzed changes in total biofilm biomass, viable cell count, and surfactin concentration over time. The results revealed that under static fermentation conditions, a biofilm gradually formed on the bacterial surface, undergoing dynamic changes over time. Initially appearing as a thin layer, the biofilm matured, developing increased wrinkles, enlarged pores, and a more stabilized structure (Kragh *et al.*, 2023). In later stages, the biofilm darkened in color, and its structure began to break down (Petrova *et al.*, 2016). This progression aligns with findings from previous studies (Arnaouteli *et al.*, 2021b; Sauer *et al.*, 2022), which have reported that mature biofilms provide a stable hydrophobic environment for bacterial cells. This environment facilitates enhanced oxygen availability and promotes the formation of intricate structures, including more channels and pores, to support bacterial metabolic processes.

Mature biofilms have been reported to create a stable hydrophobic environment for bacterial cells, enhancing oxygen availability within specific gradients of the biofilm and promoting the formation of finer structures, including an increased density of channels and pores (Sudagidan *et al.*, 2021). These features facilitate efficient nutrient exchange and signal transmission between cells, supporting coordinated biofilm functions (Zhou *et al.*, 2023). Biofilms have been reported to increase cell viability in response to different biotic and abiotic stress conditions (Yi *et al.*, 2024). We observed that the growth rate of viable cells in the fermentation liquid was highest during the maturation period of the biofilm, with slower growth rates during the early and late stages. The production of surfactin A has been observed to increase under conditions of high cell density within biofilms and nutrient limitation.

This induction is likely linked to bacterial stress responses. Across the phylogenetic tree, bacteria are known to modulate the synthesis of bacteriocins and antibiotics through stress-response pathways that detect nutrient deprivation and cellular damage (Cornforth *et al.*, 2013). The exact correlation between stress responses and surfactin A production should be further investigated.

The addition of metal ion promoters such as  $Mg^{2+}$ ,  $K^+$ , and  $Mn^{2+}$  has been reported to enhance both biomass and surfactin yield during fermentation (Gancel *et al.*, 2009). In this study, surfactin production was directly correlated with the number and physiological state of viable cells, as objectively demonstrated by the time course of surfactin yield. Notably, in industrial production, the use of liquid distributors to regulate biofilm distribution, as opposed to traditional stirred-tank bioreactors, has been shown to effectively mitigate foam formation while significantly enhancing surfactin synthesis (Zune *et al.*, 2017).

QS mechanisms are widespread in microorganisms, and the ComQXPA system (Bareia *et al.*, 2018) is a common QS system in *B. subtilis*. Cao *et al.* (2024) performed a transcriptomic analysis of *Bacillus amyloliquefaciens* HM618, revealing that the ComQXPA system plays a positive regulatory role in fengycin production. To explore the role of the ComQXPA system in *B. subtilis* ASAG 010, particularly its impact on biofilm formation and surfactin synthesis, we focused on one of its key effector molecules, ComA. A mutant strain with the *ComA* gene deleted ( $\Delta ComA$ ) was constructed. The results demonstrated that the total biofilm biomass of the  $\Delta ComA$  strain was significantly reduced compared to the wild-type strain. Further analysis of the biofilm matrix revealed that the main component of the biofilm, extracellular polysaccharides (Vandana *et al.*, 2022), were significantly reduced, along with protein content and another extracellular component, Y-PGA (Yu *et al.*, 2016), required for biofilm formation. Among the proteins involved in biofilm formation, BslA plays a critical

role in forming the outer surface of the biofilm, contributing to its hydrophobic wrinkles and overall volume (Hobley *et al.*, 2013) TasA, another key protein, protects the hydrophobic surface of the biofilm (Diehl *et al.*, 2018). RT-qPCR analysis revealed that the expression levels of *eps* and *BsIA* were significantly downregulated in the  $\Delta ComA$  strain, supporting the observed phenotypic changes at the genetic level. In contrast, the expression of TasA remained largely unchanged, potentially indicating that *ComA* does not regulate this protein. Consequently, surfactin production was significantly reduced in the mutant strain compared to the wild-type, with alterations in biofilm formation identified as a major contributing factor.

ComA has been identified as a key regulatory element in *B. velezensis* NAU-B3, where it governs surfactin synthesis and spore formation (Liang *et al.*, 2020). To investigate whether *ComA* in *B. subtilis* ASAG 010 directly influences surfactin production, a DNA pull-down assay was performed. The results revealed that heterologously expressed ComA binds specifically to the surfactin promoter, directly linking the QS effector molecule ComA from the ComQXPA system to the regulation of surfactin expression.

Interestingly, ComA's regulatory influence extends beyond surfactin. It can also bind to the *cesB* promoter, initiating carboxylesterase expression (Xiao *et al.*, 2020). Overexpression of *comA* in *B. subtilis* HND2-3 significantly enhanced lipopeptide production (Wang *et al.*, 2024). This multifaceted regulatory role is attributed to ComA's unique helix-turn-helix motif, which enables recognition of diverse topological motifs. This structural feature allows ComA to activate genes at both canonical and non-canonical sites by interacting with various RNA polymerase subunits (Wolf *et al.*, 2016). These findings underscore ComA's central role as a master regulator of both primary and secondary metabolic pathways in *Bacillus* species.

*ComA* also competes with negative regulatory proteins to enhance surfactin synthesis. For instance, the master regulator *Spo0A* has been shown to negatively control surfactin production, with its deletion significantly increasing surfactin yields (Klausmann *et al.*, 2021). The *CodY* protein inhibits *srfAA-AD* transcription by competing with the RNA polymerase binding site in the *srfAA* promoter region (Chumsakul *et al.*, 2011). Knockout of the *CodY* gene resulted in a 10-fold increase in surfactin production (Coutte *et al.*, 2015). *RapC* inhibited *srfAA-AD* expression by binding to *ComA* (Sun *et al.*, 2018). Therefore, the knockout of the *ComA* gene leads to an upregulation of *Spo0A*, *CodY*, and *RapC* expression to varying degrees.

## **Conclusion**

This study provides a comprehensive understanding of the intricate relationship between biofilm formation, quorum sensing, and surfactin production in *B. subtilis* ASAG 010. By employing a combination of genetic, biochemical, and molecular approaches, we demonstrated that the biofilm state plays a pivotal role in modulating surfactin synthesis. The *comA* gene, a key effector of the ComQXPA quorum-sensing system, was shown to directly regulate surfactin expression by binding to the *srfA* promoter. Additionally, we identified critical negative regulators such as *Spo0A*, *CodY*, and *RapC* that compete with *ComA* to modulate surfactin production, revealing a finely tuned regulatory network.

The findings also highlight the potential of *B. subtilis* ASAG 010 as a biocontrol agent, capable of inhibiting fungal pathogens and degrading zearalenone, with significant implications for food safety and agricultural sustainability. By bridging gaps in our understanding of biofilm-driven metabolic processes, this study sets the stage for optimizing *B. subtilis* strains for industrial applications, including enhanced lipopeptide production and biocontrol strategies. These insights pave the way for future research into engineering bacterial strains with improved biocontrol and biosynthetic capabilities

to address critical challenges in agriculture and beyond.

### **Funding**

This study was supported by the National Key Research and Development Program of China (Grant No. SQ2022YFD1300024), the National Natural Science Foundation of China (Grant No. 32372929), and the Program for Young Scholar Talents of Wenyong in Shanxi University.

### **CRedit authorship contribution statement**

Ru Jia: Conceptualization, Investigation, Resources, Data curation, Writing-Review & Editing, Supervision, Funding acquisition, Methodology; Yu Wang: Methodology, Investigation, Formal analysis, Writing-review & editing; Huachao Wang: Methodology, Data curation, Investigation, Validation; Xiao Ji: Methodology, Investigation, Data curation; Faizan Ahmed Sadiq: Writing-review & editing; Xu Wang: Investigation, Methodology; Guohua Zhang: Writing-review & editing.

### **Declaration of competing interest**

The authors declare that they have no known competing financial interests or personal relationships that could have appeared to influence the work reported in this paper.

### **Data availability**

Data will be made available on request.

### **Acknowledgments**

We would like to thank for Beijing Century Honbon Bio. Co. to provided fermentation tank.

### **References**

Arnaouteli, S., Bamford, N. C., Stanley-Wall, N. R., & Kovács, Á. T. (2021a). *Bacillus subtilis* biofilm formation and social interactions. *Nature Reviews Microbiology*, 19(9), 600-614. doi: 10.1038/s41579-021-00540-9

- Arnaouteli, S., Bamford, N. C., Stanley-Wall, N. R., & Kovács, Á. T. (2021b). *Bacillus subtilis* biofilm formation and social interactions. *Nature Reviews Microbiology*, 19(9), 600-614. doi: 10.1038/s41579-021-00540-9
- Balan, S. S., Mani, P., Kumar, C. G., & Jayalakshmi, S. (2019). Structural characterization and biological evaluation of Staphylosan (dimannooleate), a new glycolipid surfactant produced by a marine *Staphylococcus saprophyticus* SBPS-15. *Enzyme and Microbial Technology*, 120, 1-7. doi: 10.1016/j.enzmictec.2018.09.008
- Bareia, T., Pollak, S., & Eldar, A. (2018). Self-sensing in *Bacillus subtilis* quorum-sensing systems. *Nature Microbiology*, 3(1), 83-89. doi: 10.1038/s41564-017-0044-z
- Berenjian, A., Mahanama, R., Kavanagh, J., & Dehghani, F. (2015). Vitamin K series: current status and future prospects. *Critical Reviews in Biotechnology*, 35(2), 199-208. doi: 10.3109/07388551.2013.832142
- Bernat, P., Paraszkiwicz, K., Siewiera, P., Moryl, M., Płaza, G., & Chojniak, J. (2016). Lipid composition in a strain of *Bacillus subtilis*, a producer of iturin A lipopeptides that are active against uropathogenic bacteria. *World Journal of Microbiology and Biotechnology*, 32(10), 157. doi: 10.1007/s11274-016-2126-0
- Bisht, N., & Chauhan, P. S. (2020). Comparing the growth-promoting potential of *Paenibacillus lentimorbus* and *Bacillus amyloliquefaciens* in *Oryza sativa* L. var. Sarju-52 under suboptimal nutrient conditions. *Plant Physiology and Biochemistry*, 146, 187-197. doi: doi.org/10.1016/j.plaphy.2019.11.023
- Borriss, R., & Keswani, C. (2023). Biological control of the plant pathogens. *Microorganisms*, 11(12), 2930. doi: 10.3390/microorganisms11122930

- Branda, S. S., Chu, F., Kearns, D. B., Losick, R., & Kolter, R. (2006). A major protein component of the *Bacillus subtilis* biofilm matrix. *Molecular Microbiology*, 59(4), 1229-1238. doi: 10.1111/j.1365-2958.2005.05020.x
- Cao, C., Hou, Z., Ding, M., Gao, G., Qiao, B., Wei, S., & Cheng, J. (2024). Integrated biofilm modification and transcriptional analysis for improving fengycin production in *Bacillus amyloliquefaciens*. *Probiotics and Antimicrobial Proteins*. doi: 10.1007/s12602-024-10266-8
- Cappello, S., Genovese, M., Della Torre, C., Crisari, A., Hassanshahian, M., Santisi, S., & Yakimov, M. M. (2012). Effect of bioemulsificant exopolysaccharide (EPS2003) on microbial community dynamics during assays of oil spill bioremediation: A microcosm study. *Marine Pollution Bulletin*, 64(12), 2820-2828. doi: 10.1016/j.marpolbul.2012.07.046
- Cheng, Y., Lu, K., Chen, Z., Li, N., & Wang, M. (2024). Biochar Reduced the Risks of Human Bacterial Pathogens in Soil via Disturbing Quorum Sensing Mediated by Persistent Free Radicals. *Environmental Science & Technology*, 58(50), 22343-22354. doi: 10.1021/acs.est.4c07668
- Chumsakul, O., Takahashi, H., Oshima, T., Hishimoto, T., Kanaya, S., Ogasawara, N., & Ishikawa, S. (2011). Genome-wide binding profiles of the *Bacillus subtilis* transition state regulator AbrB and its homolog Abh reveals their interactive role in transcriptional regulation. *Nucleic acids research*, 39(2), 414-428. doi: 10.1093/nar/gkq780
- Cornforth, D. M., & Foster, K. R. (2013). Competition sensing: the social side of bacterial stress responses. *Nature Reviews Microbiology*, 11(4), 285-293. doi: 10.1038/nrmicro2977
- Coutte, F., Niehren, J., Dhali, D., John, M., Versari, C., & Jacques, P. (2015). Modeling leucine's metabolic pathway and knockout prediction improving the production of surfactin, a biosurfactant from *Bacillus subtilis*. *Biotechnology journal*, 10(8), 1216-1234. doi: 10.1002/biot.201400541

- Dai, C., Yan, P., Yin, X., Shu, Z., Mintah, B. K., He, R., & Ma, H. (2024). Surfactin and its antibacterial mechanism on *Staphylococcus Aureus* and application in pork preservation. *Food and Bioprocess Technology*. doi: 10.1007/s11947-024-03528-4
- Deng, Y., Chen, Z., Chen, Y., Wang, J., Xiao, R., Wang, X., & He, J. (2024). Lipopeptide C17 fengycin B exhibits a novel antifungal mechanism by triggering metacaspase-dependent apoptosis in *Fusarium oxysporum*. *Journal of Agricultural and Food Chemistry*, 72(14), 7943-7953. doi: 10.1021/acs.jafc.4c00126
- Diehl, A., Roske, Y., Ball, L., Chowdhury, A., Hiller, M., Molière, N., & Oschkinat, H. (2018). Structural changes of TasA in biofilm formation of *Bacillus subtilis*. *Proceedings of the National Academy of Sciences*, 115(13), 3237-3242. doi: 10.1073/pnas.1718102115
- Dimkić, I., Janakiev, T., Petrović, M., Degrassi, G., & Fira, D. (2022). Plant-associated *Bacillus* and *Pseudomonas* antimicrobial activities in plant disease suppression via biological control mechanisms - A review. *Physiological and Molecular Plant Pathology*, 117, 101754. doi: 10.1016/j.pmpp.2021.101754
- Ebrahimi-Zarandi, M., Saberi Riseh, R., & Tarkka, M. T. (2022). Actinobacteria as effective biocontrol agents against plant pathogens, an overview on their role in eliciting plant defense. *Microorganisms*, 10(9), 1739. doi: 10.3390/microorganisms10091739
- Fruhauf, S., Pühringer, D., Thamhesl, M., Fajtl, P., Kunz-Vekiru, E., Höbartner-Gussl, A., & Moll, W. (2024). Bacterial lactonases ZenA with noncanonical structural features hydrolyze the mycotoxin zearalenone. *ACS Catalysis*, 14(5), 3392-3410. doi: 10.1021/acscatal.4c00271
- Gancel, F., Montastruc, L., Liu, T., Zhao, L., & Nikov, I. (2009). Lipopeptide overproduction by cell immobilization on iron-enriched light polymer particles. *Process Biochemistry*, 44(9), 975-978.

- doi: 10.1016/j.procbio.2009.04.023
- Guo, M., Wu, F., Hao, G., Qi, Q., Li, R., Li, N., & Chai, T. (2017). *Bacillus subtilis* improves immunity and disease resistance in rabbits. *Frontiers in Immunology*, 8. doi: 10.3389/fimmu.2017.00354
- Harutyunyan, N., Kushugulova, A., Hovhannisyan, N., & Pepoyan, A. (2022). One health probiotics as biocontrol agents: one health tomato probiotics. *Plants*, 11(10), 1334. doi: 10.3390/plants11101334
- Hobley, L., Ostrowski, A., Rao, F. V., Bromley, K. M., Porter, M., Prescott, A. R., & Stanley-Wall, N. R. (2013). BslA is a self-assembling bacterial hydrophobin that coats the *Bacillus subtilis* biofilm. *Proceedings of the National Academy of Sciences*, 110(33), 13600-13605. doi: 10.1073/pnas.1306390110
- Jahan, I., Tai, B., Ma, J., Hussain, S., Du, H., Guo, L., & Xing, F. (2023). Identification of a Novel *Bacillus velezensis* IS-6 Nudix Hydrolase Nh-9 Involved in Ochratoxin A Detoxification by Transcriptomic Profiling and Functional Verification. *Journal of Agricultural and Food Chemistry*, 71(26), 10155-10168. doi: 10.1021/acs.jafc.3c01910
- Jensen, C. N. G., Pang, J. K. Y., Gottardi, M., Kračun, S. K., Svendsen, B. A., Nielsen, K. F., & Schulz, A. (2024). *Bacillus subtilis* promotes plant phosphorus (P) acquisition through P solubilization and stimulation of root and root hair growth. *Physiologia Plantarum*, 176(3), e14338. doi: 10.1111/ppl.14338
- Jiang, Y., Liu, Y., Zhang, X., Gao, H., Mou, L., Wu, M., & Jiang, M. (2021). Biofilm application in the microbial biochemicals production process. *Biotechnology Advances*, 48, 107724. doi: 10.1016/j.biotechadv.2021.107724

- Johns, L. E., Bebbler, D. P., Gurr, S. J., & Brown, N. A. (2022). Emerging health threat and cost of Fusarium mycotoxins in European wheat. *Nature Food*, 3(12), 1014-1019. doi: 10.1038/s43016-022-00655-z
- Kimotho, R. N., Zheng, X., Li, F., Chen, Y., & Li, X. (2024). A potent endophytic fungus *Purpureocillium lilacinum* YZ1 protects against *Fusarium* infection in field-grown wheat. *New Phytologist*, 243(5), 1899-1916. doi: 10.1111/nph.19935
- Klausmann, P., Hennemann, K., Hoffmann, M., Treinen, C., Aschern, M., Lilge, L., & Hausmann, R. (2021). *Bacillus subtilis* high cell density fermentation using a sporulation-deficient strain for the production of surfactin. *Applied Microbiology and Biotechnology*, 105(10), 4141-4151. doi: 10.1007/s00253-021-11330-x
- Kovács, Á. T. (2019). *Bacillus subtilis*. *Trends in Microbiology*, 27(8), 724-725. doi: 10.1016/j.tim.2019.03.008
- Kragh, K. N., Tolker-Nielsen, T., & Lichtenberg, M. (2023). The non-attached biofilm aggregate. *Communications Biology*, 6(1), 898. doi: 10.1038/s42003-023-05281-4
- Krishnan, N., Velramar, B., & Velu, R. K. (2019). Investigation of antifungal activity of surfactin against mycotoxigenic phytopathogenic fungus *Fusarium moniliforme* and its impact in seed germination and mycotoxicosis. *Pesticide Biochemistry and Physiology*, 155, 101-107. doi: 10.1016/j.pestbp.2019.01.010
- Lahlali, R., Ezrari, S., Radouane, N., Kenfaoui, J., Esmael, Q., El Hamss, H., & Barka, E. A. (2022). Biological Control of Plant Pathogens: A Global Perspective. *Microorganisms*, 10(3), 596. doi: 10.3390/microorganisms10030596
- Li, S., Hu, J., Ning, S., Li, W., Jiang, R., Huang, J., & Li, Y. (2024). *Bacillus velezensis* HY19 as a

- sustainable preservative in post-harvest citrus (*Citrus reticulata* Blanco L.) fruit management. *Food Control*, 155, 110068. doi: 10.1016/j.foodcont.2023.110068
- Liang, C., Xi-xi, X., Yun-xiang, S., Qiu-hua, X., Yang-yong, L., Yuan-sen, H., & Ke, B. (2023). Surfactin inhibits *Fusarium graminearum* by accumulating intracellular ROS and inducing apoptosis mechanisms. *World Journal of Microbiology and Biotechnology*, 39(12), 340. doi: 10.1007/s11274-023-03790-2
- Liang, Z., Qiao, J., Li, P., Zhang, L., Qiao, Z., Lin, L., & Gao, X. (2020). A novel Rap-Phr system in *Bacillus velezensis* NAU-B3 regulates surfactin production and sporulation via interaction with ComA. *Applied Microbiology and Biotechnology*, 104(23), 10059-10074. doi: 10.1007/s00253-020-10942-z
- Liu, D., Chen, Y., Ding, F., Zhao, T., Wu, J., Guo, T., & Ying, H. (2014). Biobutanol production in a *Clostridium acetobutylicum* biofilm reactor integrated with simultaneous product recovery by adsorption. *Biotechnology for Biofuels*, 7(1), 5. doi: 10.1186/1754-6834-7-5
- Liu, Y., Liu, L., Huang, Z., Guo, Y., Tang, Y., Wang, Y., & Zhao, L. (2024). Combined Strategies for Improving Aflatoxin B1 Degradation Ability and Yield of a *Bacillus licheniformis* CotA-Laccase. *International Journal of Molecular Sciences*, 25(12), 6455. doi: 10.3390/ijms25126455
- Miao, H., Xiang, X., Cheng, L., Wu, Q., & Huang, Z. (2024). New insights into the efficient secretion of foreign protein in *Bacillus subtilis* via Ribo-seq and RNA-seq integrative analyses. *BMC Microbiology*, 24(1), 537. doi: 10.1186/s12866-024-03700-y
- Nguyen, T., Chen, X., Ma, L., & Feng, Y. (2024). Mycotoxin Biodegradation by *Bacillus* Bacteria—A Review. *Toxins*, 16(11), 478. doi: 10.3390/toxins16110478
- Peng, X., Zhang, D., Yuan, J., Yang, H., Li, M., Zhang, H., & Ying, H. (2024). Engineering bacterium

- for biofilm formation and L-lysine production in continuous fermentation. *Bioresource Technology*, 414, 131567. doi: 10.1016/j.biortech.2024.131567
- Petrova, O. E., & Sauer, K. (2016). Escaping the biofilm in more than one way: desorption, detachment or dispersion. *Current opinion in microbiology*, 30, 67-78. doi: 10.1016/j.mib.2016.01.004
- Pyoung, I. K., Jaewon, R., & Young, H. K. (2010). Production of Biosurfactant Lipopeptides Iturin A, Fengycin and Surfactin A from *Bacillus subtilis* CMB32 for Control of *Colletotrichum gloeosporioides*. *Journal of Microbiology and Biotechnology*, 20(1), 138-145. doi: 10.4014/jmb.0905.05007
- Reuter, K., Mofid, M. R., Marahiel, M. A., & Ficner, R. (1999). Crystal structure of the surfactin synthetase - activating enzyme Sfp: a prototype of the 4' - phosphopantetheinyl transferase superfamily. *The EMBO Journal*, 18(23), 6823-6831. doi: 10.1093/emboj/18.23.6823
- Reveglia, P., Corso, G., & Evidente, A. (2024). Advances on Bioactive Metabolites with Potential for the Biocontrol of Plant Pathogenic Bacteria. *Pathogens*, 13(11), 1000. doi: 10.3390/pathogens13111000
- Sadiq, F. A., Yan, B., Zhao, J., Zhang, H., & Chen, W. (2020). Untargeted metabolomics reveals metabolic state of *Bifidobacterium bifidum* in the biofilm and planktonic states. *LWT*, 118, 108772. doi:10.1016/j.lwt.2019.108772
- Sarwar, A., Hassan, M. N., Imran, M., Iqbal, M., Majeed, S., Brader, G., & Hafeez, F. Y. (2018). Biocontrol activity of surfactin A purified from *Bacillus* NH-100 and NH-217 against rice bakanae disease. *Microbiological Research*, 209, 1-13. doi: 10.1016/j.micres.2018.01.006
- Sauer, K., Stoodley, P., Goeres, D. M., Hall-Stoodley, L., Burmølle, M., Stewart, P. S., & Bjarnsholt, T. (2022). The biofilm life cycle: expanding the conceptual model of biofilm formation. *Nature*

- Reviews Microbiology, 20(10), 608-620. doi: 10.1038/s41579-022-00767-0
- Shao, H., Su, X., Wang, Y., Zhang, J., Tu, T., Wang, X., & Qin, X. (2024). Oxidative degradation and detoxification of multiple mycotoxins using a dye-decolorizing peroxidase from the white-rot fungus *Bjerkandera adusta*. LWT, 206, 116597. doi: 10.1016/j.lwt.2024.116597
- Sudagidan, M., Ozalp, V. C., Öztürk, O., Yurt, M. N. Z., Yavuz, O., Tasbasi, B. B., & Aydin, A. (2021). Bacterial surface, biofilm and virulence properties of *Listeria monocytogenes* strains isolated from smoked salmon and fish food contact surfaces. Food Bioscience, 41, 101021. doi: 10.1016/j.fbio.2021.101021
- Sun, J., Qian, S., Lu, J., Liu, Y., Lu, F., Bie, X., & Lu, Z. (2018). Knockout of *rapC* Improves the Bacillomycin D Yield Based on De Novo Genome Sequencing of *Bacillus amyloliquefaciens* fmbJ. Journal of Agricultural and Food Chemistry, 66(17), 4422-4430. doi: 10.1021/acs.jafc.8b00418
- Sun, Y., Liu, W., Shi, X., Zheng, H., Zheng, Z., Lu, X., & Dong, Y. (2021). Inducing secondary metabolite production of *Aspergillus sydowii* through microbial co-culture with *Bacillus subtilis*. Microbial Cell Factories, 20(1), 42. doi: 10.1186/s12934-021-01527-0
- Thambugala, K. M., Daranagama, D. A., Phillips, A. J. L., Kannangara, S. D., & Promputtha, I. (2020). Fungi vs. Fungi in Biocontrol: An Overview of Fungal Antagonists Applied Against Fungal Plant Pathogens. Frontiers in Cellular and Infection Microbiology, 10, 604923. doi: 10.3389/fcimb.2020.604923
- van Eijk, M., Hillaire, M. L. B., Rimmelzwaan, G. F., Rynkiewicz, M. J., White, M. R., Hartshorn, K. L., & Haagsman, H. P. (2019). Enhanced Antiviral Activity of Human Surfactant Protein D by Site-Specific Engineering of the Carbohydrate Recognition Domain. Frontiers in Immunology, 10,

2476. doi: 10.3389/fimmu.2019.02476
- Vandana, & Das, S. (2022). Genetic regulation, biosynthesis and applications of extracellular polysaccharides of the biofilm matrix of bacteria. *Carbohydrate Polymers*, 291, 119536. doi: 10.1016/j.carbpol.2022.119536
- Wang, J., Ping, Y., Liu, W., He, X., & Du, C. (2024). Improvement of lipopeptide production in *Bacillus subtilis* HNDf2-3 by overexpression of the *sfp* and *comA* genes. *Preparative Biochemistry & Biotechnology*, 54(2), 184-192. doi: 10.1080/10826068.2023.2209890
- Wang, J., Xiong, Z., Fan, Y., Wang, H., An, C., Wang, B., & Wang, Y. (2024). Lignin/Surfactin Coacervate as an Eco-Friendly Pesticide Carrier and Antifungal Agent against Phytopathogen. *ACS Nano*, 18(33), 22415-22430. doi: 10.1021/acsnano.4c07173
- Wang, Y., Bian, Z., & Wang, Y. (2022). Biofilm formation and inhibition mediated by bacterial quorum sensing. *Applied Microbiology and Biotechnology*, 106(19), 6365-6381. doi: 10.1007/s00253-022-12150-3
- Wang, Y., Cong, H., Shen, Y., & Yu, B. (2025). Advances in the discovery, mechanism of action, optimization of activity and potential for clinical application of antimicrobial peptides. *Chemical Engineering Journal*, 504, 158962. doi: 10.1016/j.cej.2024.158962
- Whiteley, M., Diggle, S. P., & Greenberg, E. P. (2017). Progress in and promise of bacterial quorum sensing research. *Nature*, 551(7680), 313-320. doi: 10.1038/nature24624
- Wolf, D., Rippha, V., Mobarec, J. C., Sauer, P., Adlung, L., Kolb, P.,... Bischofs, I. B. (2016). The quorum-sensing regulator ComA from *Bacillus subtilis* activates transcription using topologically distinct DNA motifs. *Nucleic Acids Research*, 44(5), 2160-2172. doi: 10.1093/nar/gkv1242
- Wong, E. H. J., Ng, C. G., Goh, K. L., Vadivelu, J., Ho, B., & Loke, M. F. (2018). Metabolomic

- analysis of low and high biofilm-forming *Helicobacter pylori* strains. *Scientific Reports*, 8(1), 1409. doi: 10.1038/s41598-018-19697-0
- Wu, S., Qiao, J., Yang, A., & Liu, C. (2022). Potential of orthogonal and cross-talk quorum sensing for dynamic regulation in cocultivation. *Chemical Engineering Journal*, 445, 136720. doi: 10.1016/j.cej.2022.136720
- Xiao, Y., Lu, Q., Yi, X., Zhong, G., & Liu, J. (2020). Synergistic Degradation of Pyrethroids by the Quorum Sensing-Regulated Carboxylesterase of *Bacillus subtilis* BSF01. *Frontiers in Bioengineering and Biotechnology*, 8, 889. doi: 10.3389/fbioe.2020.00889
- Xu, S., Liu, Y., Cernava, T., Wang, H., Zhou, Y., Xia, T., & Chen, Y. (2022). *Fusarium* fruiting body microbiome member *Pantoea agglomerans* inhibits fungal pathogenesis by targeting lipid rafts. *Nature Microbiology*, 7(6), 831-843. doi: 10.1038/s41564-022-01131-x
- Yang, H., Li, X., Li, X., Yu, H., & Shen, Z. (2015). Identification of lipopeptide isoforms by MALDI-TOF-MS/MS based on the simultaneous purification of iturin, fengycin, and surfactin by RP-HPLC. *Analytical and Bioanalytical Chemistry*, 407(9), 2529-2542. doi: 10.1007/s00216-015-8486-8
- Yao, S., Hao, L., Zhou, R., Jin, Y., Huang, J., & Wu, C. (2022). Multispecies biofilms in fermentation: Biofilm formation, microbial interactions, and communication. *Comprehensive Reviews in Food Science and Food Safety*, 21(4), 3346-3375. doi: 10.1111/1541-4337.12991
- Yi, Y., Chen, M., Coldea, T. E., Yang, H., & Zhao, H. (2024). Soy protein hydrolysates induce menaquinone-7 biosynthesis by enhancing the biofilm formation of *Bacillus subtilis* natto. *Food Microbiology*, 124, 104599. doi: 10.1016/j.fm.2024.104599
- Yu, Y., Yan, F., Chen, Y., Jin, C., Guo, J., & Chai, Y. (2016). Poly- $\gamma$ -Glutamic Acids Contribute to

- Biofilm Formation and Plant Root Colonization in Selected Environmental Isolates of *Bacillus subtilis*. *Frontiers in Microbiology*, 7, 1811. doi: 10.3389/fmicb.2016.01811
- Zhang, N., Wang, Z., Shao, J., Xu, Z., Liu, Y., Xun, W.,... Zhang, R. (2023). Biocontrol mechanisms of *Bacillus*: Improving the efficiency of green agriculture. *Microbial Biotechnology*, 16(12), 2250-2263. doi: 10.1111/1751-7915.14348
- Zhang, Y., Qi, J., Wang, Y., Wen, J., Zhao, X., & Qi, G. (2022). Comparative study of the role of surfactin-triggered signalling in biofilm formation among different *Bacillus* species. *Microbiological Research*, 254, 126920. doi: 10.1016/j.micres.2021.126920
- Zhou, J., Wu, G., Zheng, J., Abdalmegeed, D., Wang, M., Sun, S., & Xin, Z. (2023). Research on the Regulation of Plipastatin Production by the Quorum-Sensing ComQXPA System of *Bacillus amyloliquefaciens*. *Journal of Agricultural and Food Chemistry*, 71(28), 10683-10692. doi: 10.1021/acs.jafc.3c03120
- Zhou, J., Wu, Y., Liu, D., & Lv, R. (2023). The effect of carbon source and temperature on the formation and growth of *Bacillus licheniformis* and *Bacillus cereus* biofilms. *LWT*, 186, 115239. doi: 10.1016/j.lwt.2023.115239
- Zune, Q., Telek, S., Calvo, S., Salmon, T., Alchihab, M., Toye, D., & Delvigne, F. (2017). Influence of liquid phase hydrodynamics on biofilm formation on structured packing: Optimization of surfactin production from *Bacillus amyloliquefaciens*. *Chemical Engineering Science*, 170, 628-638. doi: 10.1016/j.ces.2016.08.023



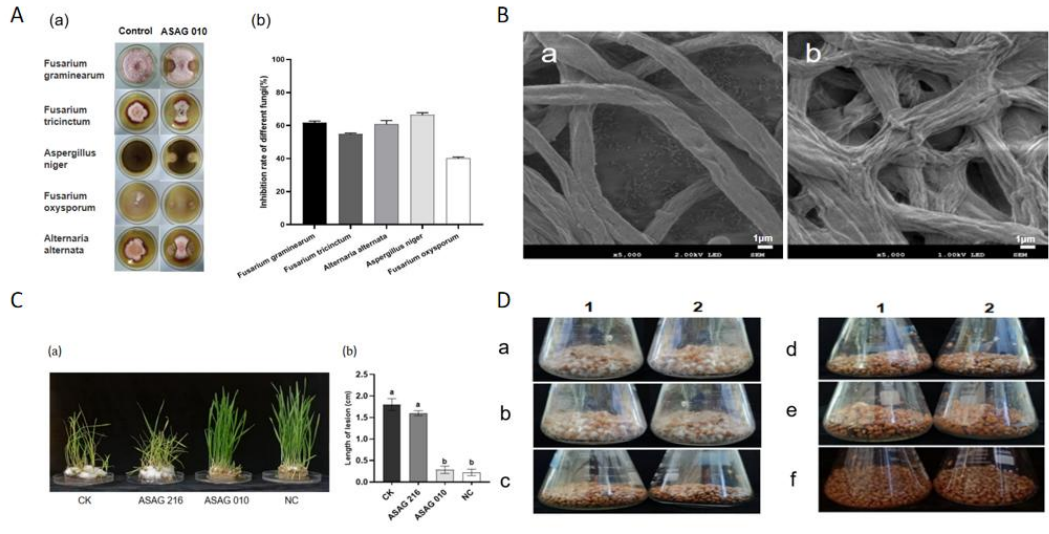


**Fig. 2. (A)** Antagonistic activity of *B. subtilis* ASAG 010 against five plant-pathogenic fungi. The inhibition rate was measured for co-cultures of *B. subtilis* ASAG 010 with *Fusarium graminearum*, *Fusarium tricinctum*, *Alternaria alternata*, *Aspergillus niger*, and *Fusarium oxysporum*. The experiment was repeated three times with consistent results. **(B)** Scanning electron microscopy (SEM) images of hyphal morphological changes in *F. graminearum* caused by treatment with *B. subtilis* ASAG 010 fermentation broth. (a) Untreated control; (b) Treated with fermentation broth. All experiments were repeated three times with consistent results. **(C)** Lesion lengths on wheat coleoptiles at 10 days post-inoculation (dpi). The experiment was repeated five times with similar results. **(D)** In vitro biocontrol effect of *B. subtilis* ASAG 010 on wheat grains. Except for group c, all groups were inoculated with 1 mL of *F. graminearum* conidia suspension (1000 CFU/mL).

- a. No further treatment.
- b. Addition of 1 mL LB liquid medium.
- c. Addition of sterile water as a negative control.
- d. Addition of 1 mL bacterial solution ( $OD_{600} = 2.0$ ).
- e. Addition of 1 mL bacterial solution ( $OD_{600} = 2.0$ ).

f. Addition of 2 mL bacterial solution ( $OD_{600} = 2.0$ ).

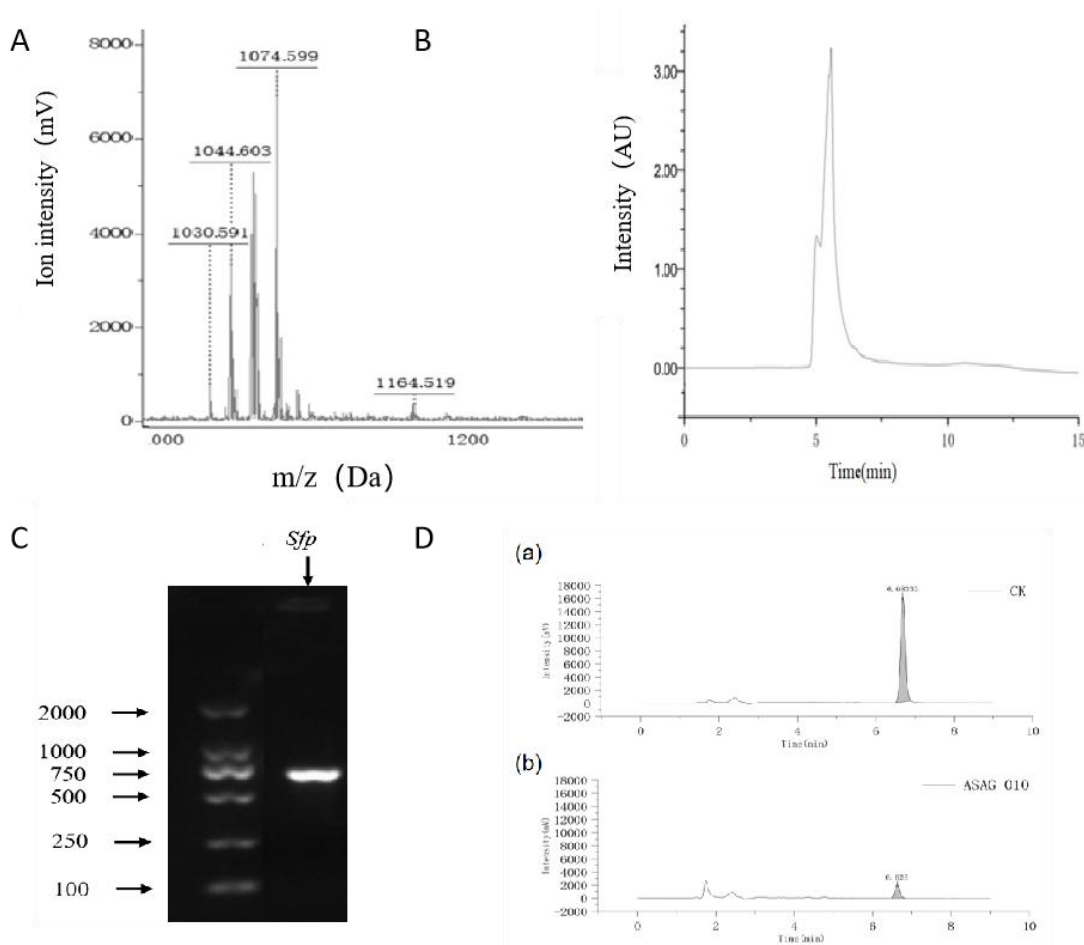


**Fig. 3.** Analysis of antimicrobial active components and degradation activity of *B. subtilis* ASAG 010. (A) MALDI-TOF-MS analysis of antimicrobial active components produced by *B. subtilis* ASAG 010 (B) HPLC chromatogram of surfactin produced by *B. subtilis* ASAG 010 (C) Agarose gel electrophoresis of the PCR product confirming the presence of the *sfp* gene associated with surfactin biosynthesis (D) HPLC analysis of zearalenone (ZEN) degradation. (a) Medium-only control group serving as a blank control; (b) Treatment group containing bacterial suspension. Both groups were incubated for 48 h under identical conditions.

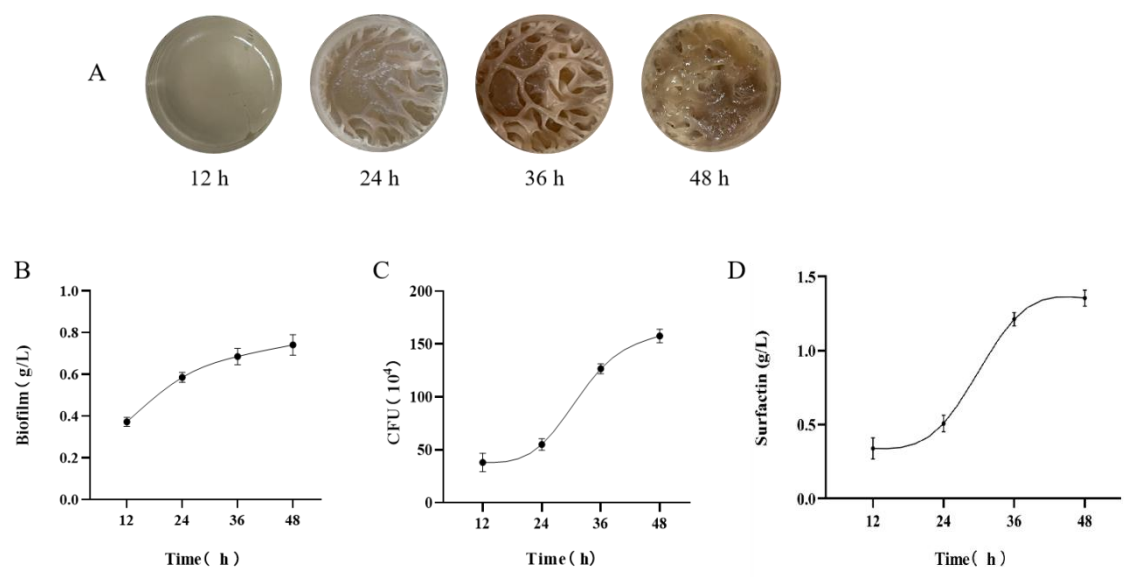


**Fig. 4.** Correlation analysis between biofilm formation and surfactin production (A) Morphological changes in the biofilm structure over time, illustrating the dynamic development and maturation of the biofilm (B) Total biofilm biomass measured at different time points (C) Viable cell count within the biofilm over time (D) Surfactin yield over time, demonstrating its correlation with biofilm formation and viable cell density.

All measurements (B, C, D) were conducted within the same experimental setup, and experiments were repeated three times with consistent results.

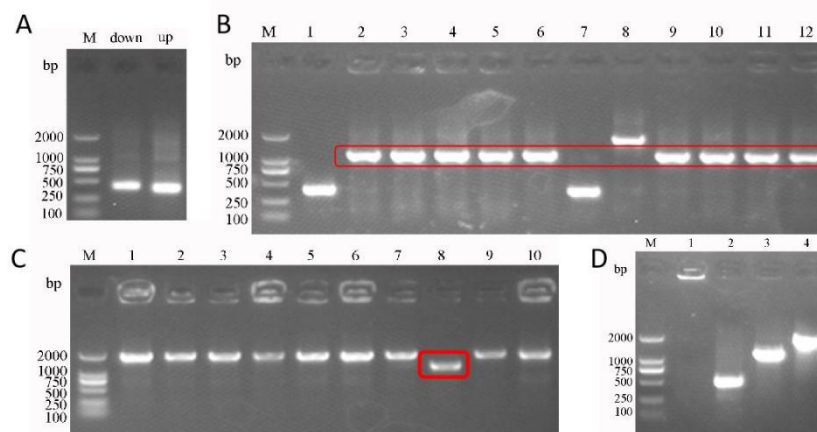


**Fig. 5.** PCR detection and identification of *ComA* gene knockout in *B. subtilis* ASAG 010. **(A)** PCR detection of the upstream and downstream homologous arms used for *ComA* gene knockout, analyzed on a 1% agarose gel. Lane M: Marker; Lane "down": downstream homologous arm; Lane "up": upstream homologous arm. **(B)** PCR identification of the *ComA* UD-sgCas9 vector, with 1-12 representing 12 randomly selected clone numbers from the plate. Clone 2 and others correspond to the correct size of the clone. **(C)** PCR identification of *ComA* gene knockout colonies. Lanes 1-10 represent randomly selected colonies, with Clone 8 displaying the correct knockout band size. **(D)** Resistance elimination identification: Lane 1 shows the amplification product of the knockout strain ASAG 010 $\Delta$ *ComA* using *ComA*-ter-F/*ComA*-ter-R primers, lane 2 is the wild-type ASAG 010 control with *ComA*-ter-F/*ComA*-ter-R primers, lane 3 shows the amplification product of the knockout strain ASAG 010 $\Delta$ *ComA* using *ComA*-JD-F/*ComA*-JD-R primers, and lane 4 is the wild-type ASAG 010 control with *ComA*-JD-F/*ComA*-JD-R primers. *ComA*-ter-F/*ComA*-ter-R: primers for the target gene; *ComA*-JD-F/*ComA*-JD-R: upstream arm + target gene + downstream arm.

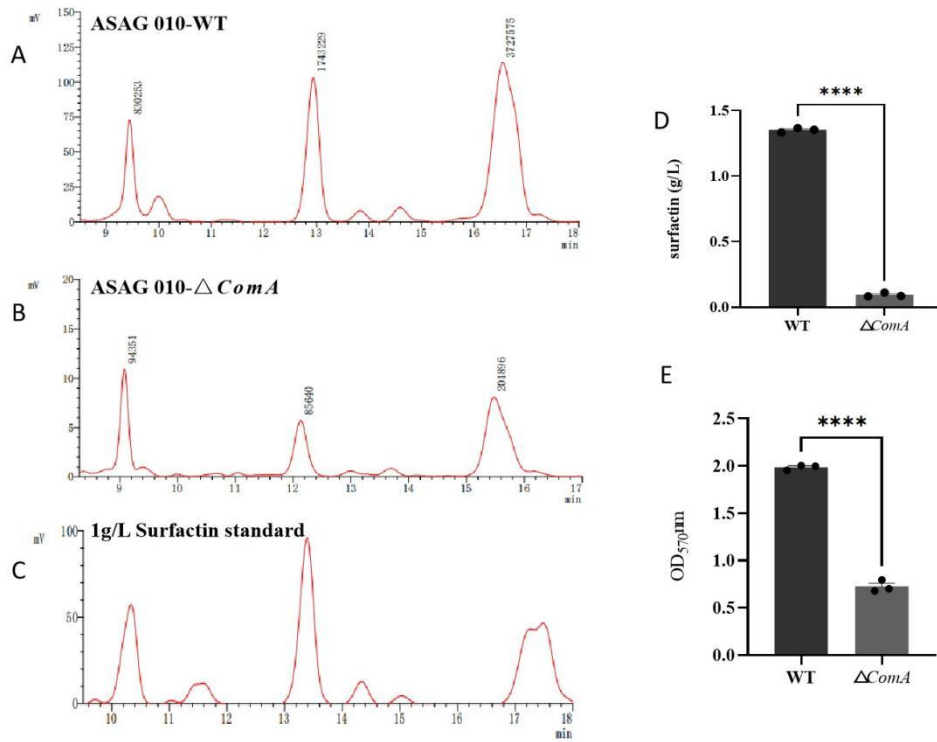


**Fig. 6.** Compare the differences in surfactin production and biofilm total between wild-type and mutant *B. subtilis* ASAG 010. **(A)** HPLC chart of wild-type surfactin. **(B)** HPLC chart of mutant surfactin. **(C)** HPLC chart of 1 g/L surfactin standard. **(D)** Surfactin yield. **(E)** Total biofilm content (crystal violet staining method).

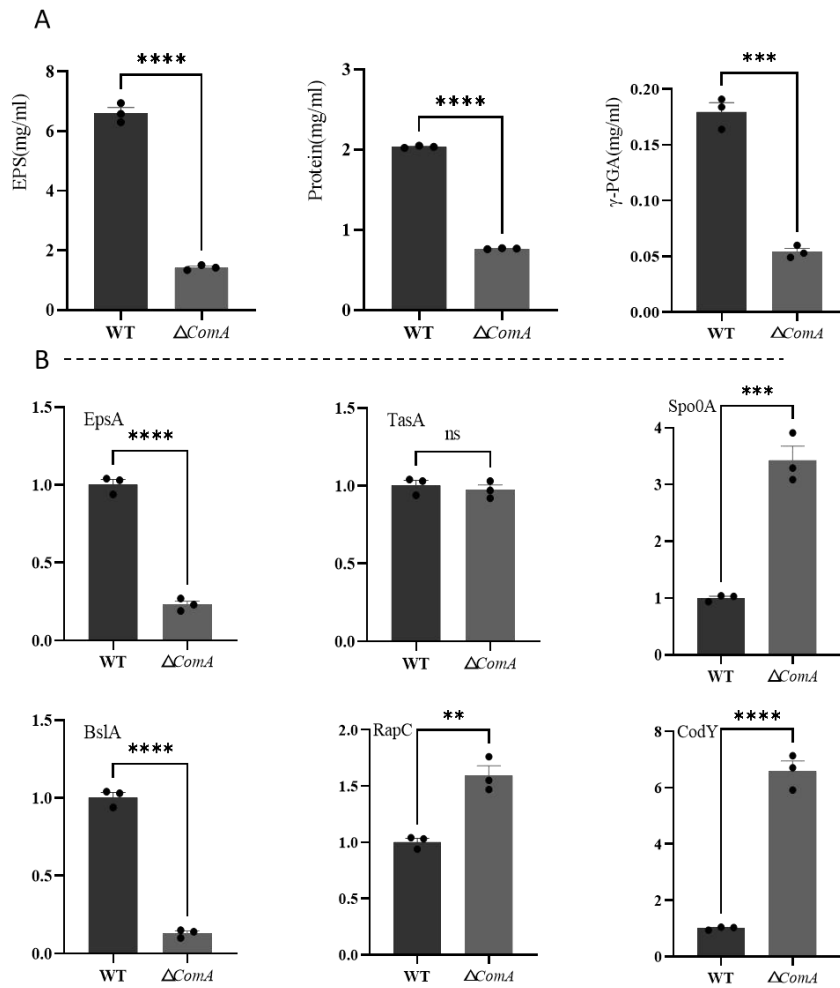


**Fig. 7.** Comparison of wild-type and *ComA*-deficient mutant *B. subtilis* ASAG 010. **(A)** Composition of biofilm matrix: EPS, Protein and  $\gamma$ -PGA. **(B)** Relative expression analysis of the genes by RT-qPCR. Data were expressed as the average of three replicate experiments, and error bars represent mean  $\pm$  SD. Asterisks indicate significant differences at the 0.01 (\*\*\*\*) level.

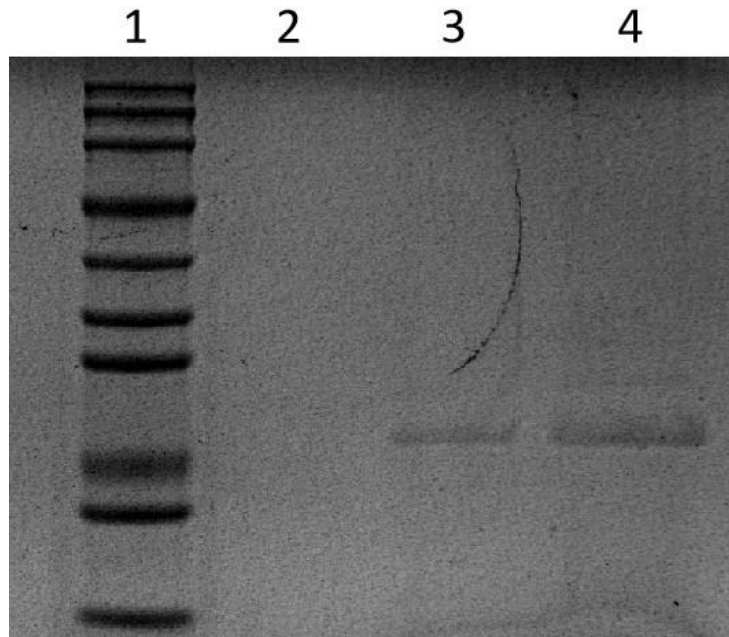


**Fig. 8.** DNA pull-down assay for validating the function of ComA protein. Lane 1: Negative control (protein + magnetic beads), Lane 2: Experimental group (probe + protein + magnetic beads), Lane 3: Positive control (only protein).